

incubation time of 30 minutes was chosen to allow for dephosphorylation of IP_3 and IP_2 to form IP_1 , while preventing further dephosphorylation of the latter by including LiCl (24). Under these conditions IP_1 accumulation served as indicator of PLC-catalyzed hydrolysis of phosphoinositides. After incubation with agonists or antagonists or both, the reaction was stopped by precipitation with trichloroacetic acid. The supernatants were extracted with diethyl ether, neutralized, and applied to Dowex-100 columns, on which inositol phosphates were separated (24).

25. The inhibition of AC-catalyzed formation of cAMP was assayed as follows: Confluent cells were harvested as in (18), washed once, and resuspended in PBS

(5×10^5 cells per milliliter). Aliquots (1 ml) were equilibrated for 20 minutes at $37^\circ C$ with $100 \mu M$ IBMX. Muscarinic agonists, antagonists, and forskolin ($10 \mu M$) were then added, and incubation was continued for 10 minutes. The cells were pelleted, resuspended in buffer, boiled for 10 minutes, and centrifuged (5 minutes, $10,000g$), and the supernatants were assayed for cAMP content by radioimmunoassay (22).

26. This work was supported by Genentech, Inc., and by NIH grants CA16417 (to J.R.) and HL23632 (to M.S.).

17 July 1987; accepted 2 October 1987

Physiological Role of Silent Receptors of Atrial Natriuretic Factor

THOMAS MAACK,* MUNEYA SUZUKI, FERNANDO A. ALMEIDA, D. NUSSENZVEIG, ROBERT M. SCARBOROUGH, GLENN A. MCENROE, JOHN A. LEWICKI

A ring-deleted analog of atrial natriuretic factor—des[Gln¹⁸, Ser¹⁹, Gly²⁰, Leu²¹, Gly²²] ANF₄₋₂₃-NH₂ (C-ANF₄₋₂₃)—binds with high affinity to approximately 99% of ANF receptors in the isolated perfused rat kidney. In this preparation, C-ANF₄₋₂₃ is devoid of detectable renal effects and does not antagonize any of the known renal hemodynamic and natriuretic actions of biologically active ANF₁₋₂₈. In contrast, both C-ANF₄₋₂₃ and ANF₁₋₂₈ increase sodium excretion and decrease blood pressure in intact anesthetized rats. This apparent contradiction is resolved by the finding that the ring-deleted analog markedly increases plasma levels of endogenous immunoreactive ANF in the rat. The results show that the majority of the renal receptors of ANF are biologically silent. This new class of receptors may serve as specific peripheral storage-clearance binding sites, acting as a hormonal buffer system to modulate plasma levels of ANF.

ADMINISTERED ATRIAL NATRIURETIC factor (ANF) has important effects on such body functions as the regulation of renal function, salt balance, plasma volume, and blood pressure (1). Many, if not all, of these actions, are assumed to be mediated by guanosine 3',5'-monophosphate (cGMP), which is generated as ANF interacts with its biological receptors (B-ANF receptors) (2). Specific high-affinity binding sites of ANF have been described in several tissues; in kidney they are localized mainly in vascular and glomerular structures of the cortex (1-3). Recent studies in the isolated perfused rat kidney show a remarkable identity between the specific binding curve of ANF in the kidney cortex and the dose-response curves of such renal effects of the hormone as increase in glomerular filtration rate (GFR), increase in urinary excretion of fluid and electrolytes, and vasorelaxation of precontracted renal

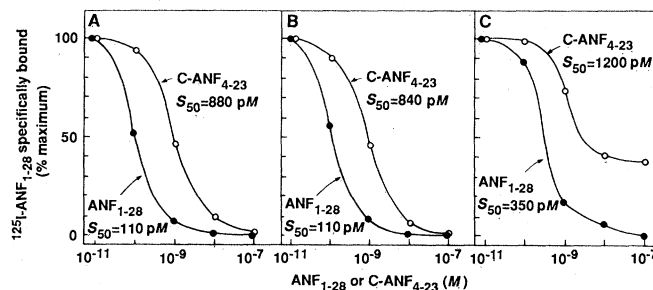
vasculature (4). There are, however, major discrepancies between the kinetics of ANF-specific binding and the dose-response curve of its effect on cGMP accumulation (2, 5). Furthermore, in vascular smooth muscle and endothelial cells in culture, some analogs of ANF that effectively compete for specific binding sites are very weak agonists and do not antagonize the ANF-induced increase in cGMP (6). These data raise the possibility that either cGMP is not the sole mediator of ANF actions or that there is a separate class

of biologically silent ANF receptors (C-ANF receptors).

In this report we address the question of whether there is a significant number of C-ANF receptors in the kidney and explore the issue of the physiological role of these receptors. For these purposes we used a combined *in vitro*-*in vivo* approach, which relates specific binding curves to the functional effects of biologically active ANF₁₋₂₈ (7) and of the ring-deleted analog C-ANF₄₋₂₃ (des[Gln¹⁸, Ser¹⁹, Gly²⁰, Leu²¹, Gly²²] ANF₄₋₂₃-NH₂) (8). These peptides were chosen because ANF₁₋₂₈ is the natural form of biologically active ANF (7), whereas C-ANF₄₋₂₃ competes effectively with biologically active atrial peptides for binding sites but is devoid of agonist or antagonist action on the generation of cGMP in vascular smooth muscle and endothelial cells in culture (9).

C-ANF₄₋₂₃ effectively competed for the overwhelming majority of specific binding sites of ¹²⁵I-labeled ANF₁₋₂₈ in isolated perfused rat kidney (Table 1 and Fig. 1). This analog ($10^{-7}M$) almost completely inhibited the specific binding of ¹²⁵I-labeled ANF₁₋₂₈ to whole-kidney tissue, cortex, and inner stripe of the outer medulla. From these data it can be estimated that C-ANF₄₋₂₃ can occupy close to 99% of the binding sites of ANF in these kidney regions (Table 1). In the renal papilla, which contains less than 2% of the total binding sites of ANF₁₋₂₈ in the kidney (4), C-ANF₄₋₂₃ bound to a lesser extent than ANF₁₋₂₈ but still was able to occupy approximately 60% of the specific binding sites of ¹²⁵I-labeled ANF₁₋₂₈ (Table 1, Fig. 1C). The apparent affinities of C-ANF₄₋₂₃ (expressed as S_{50} , the perfusate concentration of the peptide required to decrease the specific binding of ¹²⁵I-labeled ANF₁₋₂₈ to half the maximal level) for binding sites in whole-kidney tissue and kidney cortex were very high, albeit about eightfold lower than the corresponding apparent affinities of ANF₁₋₂₈ (Fig. 1, A and B).

Fig. 1. Competition for binding between ¹²⁵I-labeled ANF₁₋₂₈ and ANF₁₋₂₈ or the ring-deleted analog C-ANF₄₋₂₃ in whole-kidney tissue (A), cortex (B), and papilla (C) in isolated perfused rat kidney. Kidneys were perfused in a closed-circuit system in the nonfiltering mode as described (16). ¹²⁵I-labeled ANF₁₋₂₈ (4 pM) and the concentrations of ANF₁₋₂₈ or C-ANF₄₋₂₃ indicated on the abscissas were added together to the perfusate at the beginning of the perfusion. After 50 minutes, perfusion was terminated and specific binding of ¹²⁵I-labeled ANF₁₋₂₈ to whole-kidney tissue, cortex, and papilla was determined as described (Table 1) (4). Results (average of two kidneys per concentration point) are expressed as percentage of maximal specific binding (ordinate) against perfusate concentration of peptides (abscissa). S_{50} , perfusate concentration of peptide required to decrease specific binding of ¹²⁵I-labeled ANF₁₋₂₈ to half the maximal level.



T. Maack, M. Suzuki, F. A. Almeida, D. Nussenzveig, Department of Physiology, Cornell University Medical College, New York, NY 10021.
R. M. Scarborough, G. A. McEnroe, J. A. Lewicki, California Biotechnology, Inc., Mountain View, CA 94043.

*To whom all correspondence should be addressed.

At maximal occupancy of binding sites in the isolated perfused rat kidney, C-ANF₄₋₂₃ (10⁻⁷M) was devoid of any of the known effects of ANF on GFR (Fig. 2A), sodium excretion ($U_{Na}V$, where U_{Na} is the concentration of sodium in urine and V is the urine flow rate) (Fig. 2B), renal vascular resistance, filtration fraction, urine flow rate, potassium excretion, or vasorelaxation of precontracted kidneys (10). Even at maximal receptor occupancy, C-ANF₄₋₂₃ did not antagonize the ANF₁₋₂₈-induced effects on GFR (Fig. 2A), on $U_{Na}V$ (Fig. 2B), or on

the other parameters referred to above (10). There was a tendency for a small potentiation of the effects of ANF₁₋₂₈ in the presence of C-ANF₄₋₂₃, but the difference did not reach statistical significance (Fig. 2) (11).

Thus, C-ANF₄₋₂₃ shares with ANF₁₋₂₈ close to 99% of the specific binding sites of ANF in kidney tissue. Since the S_{50} of binding to the renal cortex and the ED_{50} (perfusate concentration of peptide required to elicit half-maximal effect) of the renal effects of ANF₁₋₂₈ were very similar (Figs. 1 and 2) (4), the binding affinity of the endog-

enous form of ANF to the small proportion of B-ANF receptors must be similar to its binding affinity to C-ANF receptors (12). Furthermore, since C-ANF₄₋₂₃ had no effects on renal functions and did not antagonize any of the known renal actions of ANF₁₋₂₈, it is very likely that the overwhelming majority of the renal receptors of ANF does not mediate the renal effects of biologically active ANF₁₋₂₈ and that C-ANF₄₋₂₃ does not bind to B-ANF receptors.

In contrast to its lack of renal effects in the isolated perfused rat kidney, C-ANF₄₋₂₃ reversibly increased $U_{Na}V$ and tended to decrease blood pressure in intact anesthetized rats (Fig. 3). At a constant infusion rate of 1.0 μ g per minute per kilogram of body weight, the analog increased $U_{Na}V$ from (mean \pm SE) 1.85 \pm 0.63 to 4.22 \pm 0.80 μ Eq/min ($n = 8$, $P < 0.01$). The apparent contradiction between the lack of effect of C-ANF₄₋₂₃ in the isolated rat kidney and its effectiveness on renal and systemic functions in intact rats is most likely due to the fact that this analog markedly and reversibly increases plasma levels of endogenous immunoreactive ANF (irANF) from 51.4 \pm 9.4 to 141.7 \pm 21.1 pg/ml ($n = 8$, $P < 0.01$) (Fig. 3). Indeed, C-ANF₄₋₂₃ increased plasma irANF in each of the eight rats tested in the present experiment, the amount of increase varying between 1.5- and 6-fold. In all likelihood the increase in plasma irANF is due to a decrease in binding of endogenous hormone to C-ANF receptors, since recent studies show that C-ANF₄₋₂₃ markedly decreases the volume of distribution and the metabolic clearance rate of ¹²⁵I-labeled ANF₁₋₂₈ in intact anesthetized rats (13).

To test whether the C-ANF₄₋₂₃-induced increase in plasma irANF accounts for its natriuretic effect, we administered biologically active ANF₁₋₂₈ so as to increase plasma irANF to a value similar to that obtained with the infusion of C-ANF₄₋₂₃. ANF₁₋₂₈ (0.02 μ g per minute per kilogram of body weight) was infused into intact anesthetized rats by the same protocol as was used for C-ANF₄₋₂₃. Plasma levels of irANF increased from 118.6 \pm 7.5 to 195.4 \pm 11.3 pg/ml ($n = 5$ rats, $P < 0.01$). The latter value was not significantly different ($P > 0.05$) from that obtained during the infusion of C-ANF₄₋₂₃. $U_{Na}V$ increased from 1.86 \pm 0.74 to 3.46 \pm 1.12 μ Eq/min ($n = 5$ rats, $P < 0.01$), an increase that was also not significantly different ($P > 0.05$) from that observed with C-ANF₄₋₂₃. Thus, these results are consistent with the interpretation that the natriuretic effect of C-ANF₄₋₂₃ in intact rats is due to an increase in plasma levels of endogenous ANF.

Our results demonstrate that the over-

Fig. 2. Effects of ANF₁₋₂₈, of ring-deleted analog C-ANF₄₋₂₃, and of ANF₁₋₂₈ + C-ANF₄₋₂₃ on GFR (A) and sodium excretion (B) in isolated perfused rat kidneys. Clearance experiments in isolated rat kidneys perfused in the filtering mode were performed as described (17). The bottom part of A and B shows results of experiments in three control kidneys (●) perfused without addition of atrial peptides for the same or longer time as the experimental kidneys, and three kidneys perfused with 0.1 μ M C-ANF₄₋₂₃ alone (○). C-ANF₄₋₂₃ was added to the perfusate after control periods (C₀) followed by three 10-minute experimental clearance periods (C₁ to C₃). The top part of A and B shows results of experiments in four kidneys perfused with increasing concentrations of ANF₁₋₂₈ alone (▲), and four kidneys perfused with increasing concentrations of ANF₁₋₂₈ in presence of 0.1 μ M C-ANF₄₋₂₃ (□). C-ANF₄₋₂₃ was added before the control periods (C₀). The perfusate concentrations of ANF₁₋₂₈ are shown in abscissas of the top part of A and B. After the addition of ANF₁₋₂₈ to give the perfusate concentrations shown in the abscissas, a 5-minute equilibration was allowed before a 5-minute clearance period. Results (mean \pm SE) are expressed as differences between experimental and C₀ periods. Mean \pm values for GFR and sodium excretion ($U_{Na}V$) in C₀ periods (14 kidneys) were 0.53 \pm 0.04 ml/min and 0.34 \pm 0.05 μ Eq/min, respectively, and did not differ significantly ($P > 0.05$) among the four groups of isolated kidneys. GFR was determined by the clearance of [¹⁴C]inulin, and Na was determined by flame photometry (17). ED_{50} , perfusate concentration of peptide required to elicit half-maximal effect.

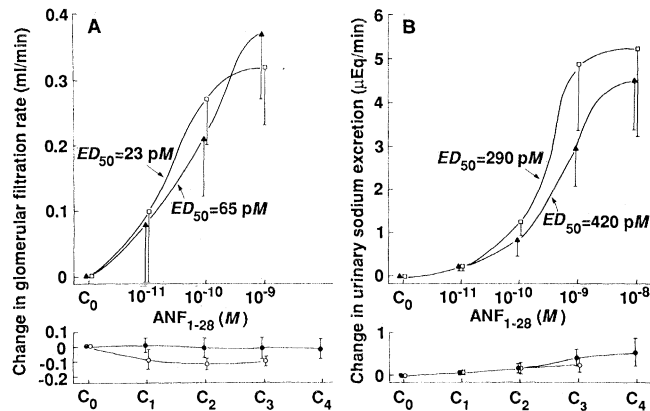
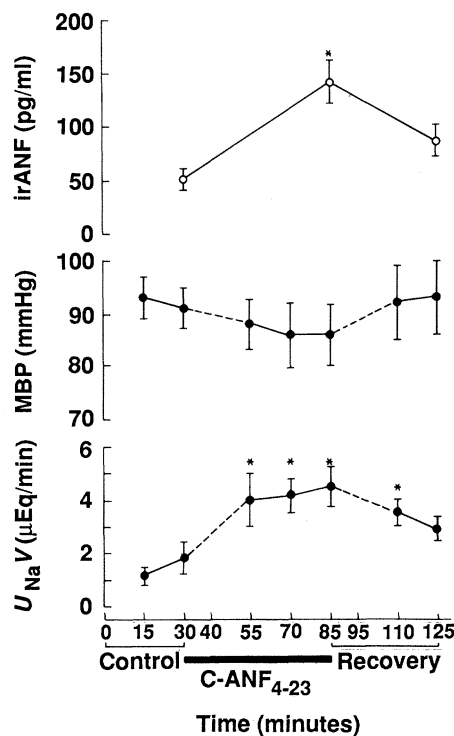


Table 1. Specific binding of ¹²⁵I-labeled ANF₁₋₂₈ to whole-kidney tissue, cortex, outer medulla, and papilla in isolated perfused rat kidney: competition with ANF₁₋₂₈ and C-ANF₄₋₂₃. Isolated rat kidneys were perfused in a closed-circuit system at 37°C in the nonfiltering mode as described (16). ¹²⁵I-labeled ANF₁₋₂₈ (0.5 μ Ci, 4 pM) was added to the perfusate alone (four kidneys) or with 0.1 μ M ANF₁₋₂₈ (eight kidneys) or 0.1 μ M of the ring-deleted analog C-ANF₄₋₂₃ (four kidneys). After 50 minutes of perfusion, a time at which near-equilibrium perfusate concentrations of ¹²⁵I-labeled ANF₁₋₂₈ were attained and accumulation in kidney was maximal (4), perfusion was terminated. The kidneys were briefly washed, weighed, and small pieces of cortex, inner stripe of outer medulla, and papilla were removed, weighed, and counted for ¹²⁵I radioactivity (4). The amount of ¹²⁵I-labeled ANF₁₋₂₈ specifically bound to whole-kidney tissue and its sections was calculated as the difference between total and nonspecifically bound ¹²⁵I. The latter is defined as binding of ¹²⁵I in presence of 1 μ M ANF₁₋₂₈ and accounts for less than 1% of total maximal binding of ¹²⁵I (4). End perfusate samples were precipitated with trichloroacetic acid (TCA) and counted for ¹²⁵I radioactivity (4). A previous study (4) showed that: (i) perfusate concentration of TCA-precipitated (ppt) ¹²⁵I fairly represents that of unlabeled ANF₁₋₂₈; (ii) accumulation of label in kidney tissue is due to binding to surface membranes, since it also occurs when kidneys are perfused at 4°C and since the binding is reversible by perfusion with acid solution; and (iii) bound radioligand removed by acid perfusion coelutes with ¹²⁵I-labeled ANF₁₋₂₈ on reversed-phase HPLC. Results (mean \pm SE) are expressed as cpm specifically bound [¹²⁵I] radioactivity per gram of tissue divided by cpm TCA ppt ¹²⁵I radioactivity per milliliter of perfusate.

Tissue portion	Tissue [¹²⁵ I-ANF ₁₋₂₈]/perfusate [¹²⁵ I-ANF ₁₋₂₈]		
	¹²⁵ I-ANF ₁₋₂₈	¹²⁵ I-ANF ₁₋₂₈ + ANF ₁₋₂₈	¹²⁵ I-ANF ₁₋₂₈ + C-ANF ₄₋₂₃
Whole kidney	123 \pm 19	0.10 \pm 0.02	1.3 \pm 0.1
Cortex	161 \pm 13	0.12 \pm 0.02	1.7 \pm 0.1
Outer medulla	22 \pm 5	0.07 \pm 0.03	1.1 \pm 0.3
Papilla	15 \pm 6	0.13 \pm 0.05	2.8 \pm 0.2

Fig. 3. Effects of ring-deleted analog of ANF (C-ANF₄₋₂₃) on sodium excretion ($U_{Na}V$), mean arterial blood pressure (MBP), and plasma concentration of endogenous immunoreactive ANF (irANF) in anesthetized rats. Clearance experiments were performed in Sprague-Dawley rats that had been anesthetized with Inactin (100 mg per kilogram of body weight), as described (18). After control periods, C-ANF₄₋₂₃ was administered intravenously as a bolus injection (10 μ g per kilogram of body weight) followed by a constant infusion (1 μ g min⁻¹ per kilogram of body weight). A 10-minute equilibration period was allowed followed by three 15-minute experimental clearance periods. Fifteen minutes after the infusion was stopped, there were two 15-minute recovery clearance periods. Blood pressure was monitored continuously with a pressure transducer connected to the carotid artery. For radioimmunoassay (RIA) of ANF, 2 ml of blood were withdrawn from the carotid artery immediately before the first control period and at the end of the last experimental and recovery periods. Fresh blood (2 ml) obtained from littermates was infused intravenously to replace each blood sampling. Results are means \pm SE of eight rats; * P < 0.01 versus control periods, paired Student's t test. RIA of ANF was performed as described (19, 20). Blood samples were collected in chilled Vacutainer tubes containing potassium EDTA. The tubes were centrifuged, and the plasma was stored at -70°C until assayed. Plasma samples, containing 1000 cpm of ¹²⁵I-ANF₁₋₂₈ to determined recovery ($60 \pm 4\%$ SD), were extracted by filtration through C₁₈ Sep-Pak cartridges (Waters Associates) (19). Reconstituted samples (0.1 ml) were assayed for ANF with the α -human ANF RIA kit from Peninsula Laboratories Inc. C-ANF₄₋₂₃ at concentrations up to 100 ng/ml plasma was completely devoid of cross-reactivity with the antibody.



whelming majority of the renal receptors of ANF are biologically silent, since they do not mediate any of the known renal effects of the hormone. C-ANF receptors in the kidney may be identical to ANF receptors in vascular smooth muscle and endothelium, which do not mediate the ANF-induced increase in cGMP (6, 9). Although it cannot be ruled out that C-ANF receptors may relay a yet unknown physiological effect of the hormone that is not mediated by cGMP, the present results suggest that they serve as specific storage-clearance binding sites of the hormone. The results of the in vivo experiments strongly support this hypothesis since C-ANF₄₋₂₃ markedly increases plasma levels of endogenous ANF in anesthetized rats. The results of the in vitro and in vivo experiments indicate that occupancy of C-ANF receptors by C-ANF₄₋₂₃ decreases binding of ANF₁₋₂₈ to these receptors. Consequently, plasma levels of endogenous ANF increase, a phenomenon that in turn explains the natriuretic and blood pressure-lowering effect of C-ANF₄₋₂₃ in intact rats.

Although some biological effects of ANF may be mediated by secondary messengers other than cGMP, our results suggest that observed discrepancies between binding of atrial peptides and generation of cGMP (6) are due to the large proportion of biologically silent receptors of this hormone in kidney and perhaps other tissues. Conse-

quently, in studies on characterization of ANF receptors by cross-linking techniques and purification of ANF receptors, attention must be given to the very large proportion of C-ANF receptors as compared to B-ANF receptors in various tissues (14). In studies on receptor regulation it is important to test which of the receptors is being regulated since, for example, down-regulation of C-ANF receptors would lead to physiological consequences that are opposite to those of down-regulation of B-ANF receptors.

In view of their large number in kidney and perhaps other tissues, C-ANF receptors may account for the very large volume of distribution and high metabolic clearance rate of ANF in the rat (13, 15). Consequently, C-ANF receptors may act as a hormonal buffer system impeding large inappropriate fluctuations of the plasma levels of this hormone. Conversely, as demonstrated in the present study, it becomes possible to increase plasma levels of endogenous ANF by decreasing its binding to C-ANF receptors with agonists that bind to C-ANF but not to B-ANF receptors, such as C-ANF₄₋₂₃.

REFERENCES AND NOTES

1. For reviews on atrial natriuretic factor see: A. J. de Bold, *Science* **230**, 767 (1985); T. Maack *et al.*, *Kidney Int.* **27**, 607 (1985); P. Needleman *et al.*, *Hypertension (Dallas)* **7**, 469 (1985); T. Maack, in *Physiologie Aktuell*, B. Bromm and D. W. Lubbers, Eds. (Gustav Fisher Verlag, New York, 1986), vol.

- 2, pp. 51-85.
2. S. A. Waldman, R. M. Rapoport, F. Murad, *J. Biol. Chem.* **259**, 14332 (1984); R. J. Winquist *et al.*, *Proc. Natl. Acad. Sci. U.S.A.* **81**, 7661 (1984); P. Hamet *et al.*, *Biochem. Biophys. Res. Commun.* **123**, 515 (1984); Y. Hirata *et al.*, *ibid.* **125**, 562 (1984); D. B. Schenk *et al.*, *ibid.* **127**, 433 (1985).
3. M. A. Napier *et al.*, *Proc. Natl. Acad. Sci. U.S.A.* **81**, 5946 (1984); C. Bianchi, J. Gutkowska, S. Genest, M. Cantin, *Histochemistry* **82**, 441 (1985).
4. M. Suzuki *et al.*, *Am. J. Physiol.* **253**, F917 (1987).
5. B. J. Ballerman, R. L. Hoover, M. J. Karnowski, B. M. Brenner, *J. Clin. Invest.* **76**, 2049 (1985).
6. D. C. Leitman and F. Murad, *Biochim. Biophys. Acta* **885**, 74 (1986); R. M. Scarborough *et al.*, *J. Biol. Chem.* **261**, 12960 (1986).
7. The nomenclature of ANF used in the present article takes the 28-amino acid COOH-terminal sequence of pro-ANF as the basic atrial peptide since this peptide is the predominant form of smaller atrial peptides in atria and in circulating blood (1) [D. Schwartz *et al.*, *Science* **229**, 397 (1985)]. The amino acid sequence of rat ANF₁₋₂₈ is: Ser-Leu-Arg-Arg-Ser-Ser-Cys-Phe-Gly-Gly-Arg-Ile-Asp-Arg-Ile-Gly-Ala-Gln-Ser-Gly-Leu-Gly-Cys-Asn-Ser-Phe-Arg-Tyr, with a disulfide bridge between the cysteines (1).
8. The amino acid sequence of C-ANF₄₋₂₃ is: Arg-Ser-Ser-Cys-Phe-Gly-Gly-Arg-Ile-Asp-Arg-Ile-Gly-Ala-Cys-NH₂, with a disulfide bridge between the cysteines. This compound was prepared by means of standard solid-phase peptide synthetic protocols as described (6). The crude peptide cleaved from the resin with hydrogen fluoride was cyclized in dilute solution of K₃Fe(CN)₆ (10 mM). The resulting disulfide-bridged peptide was purified by gel filtration (G-25, 0.5M HOAc), ion-exchange (CM-cellulose) chromatography and semipreparative reversed-phase high-performance liquid chromatography (HPLC). The pure peptide was characterized by amino acid analysis and gas-phase amino-terminal sequence analysis (Applied Biosystems).
9. R. M. Scarborough *et al.*, in *Proceedings and Abstracts of the Second World Congress of Biologically Active Atrial Peptides*, American Society of Hypertension, New York, 16 to 21 May 1987 (American Society of Hypertension, New York, 1987), p. 190.
10. A summary of the data on the effects of ANF₁₋₂₈, C-ANF₄₋₂₃, and ANF₁₋₂₈ in the presence of C-ANF₄₋₂₃ on all renal function parameters of the isolated perfused rat kidney determined in the present study (renal vascular resistance, GFR, filtration fraction, urine flow, absolute and fractional urinary excretion of sodium and potassium, and vasorelaxation of kidneys precontracted with the addition of renin substrate to the perfusate) is available to interested investigators upon written request to the authors.
11. A relatively small potentiating effect of C-ANF₄₋₂₃ on the renal effects of ANF₁₋₂₈ could be expected in view of higher perfusate equilibrium concentrations of ANF₁₋₂₈ when kidneys are perfused with high concentrations of the analog. Indeed, at the lowest initial perfusate concentrations of ANF₁₋₂₈ (10^{-11} to 10^{-9} M), in the absence of C-ANF₄₋₂₃, the final equilibrium perfusate concentrations of ANF₁₋₂₈ at 50 minutes of perfusion are approximately 1/4 to 1/2 lower than its initial perfusate concentrations (4). This is due to ANF₁₋₂₈ binding to the very large number of C-ANF receptors in the isolated kidney. The perfusate decay of ANF₁₋₂₈ at the lowest concentrations of the peptide is prevented by excess (10^{-7} M) C-ANF₄₋₂₃ since this analog competes with ANF₁₋₂₈ for C-ANF binding sites. In view of the logarithmic nature of the dose-response curves and the variability of the measurements (Fig. 2), the expected potentiation of C-ANF₄₋₂₃ on the effects of the lowest concentrations of ANF₁₋₂₈ on renal function parameters would be too small to be statistically detectable in the isolated perfused rat kidney preparation.
12. The term C-ANF receptor is used for simplicity, since we cannot determine from the present data whether C-ANF receptors are a separate molecular entity from B-ANF receptors or a separate specific binding site on the B-ANF receptor. Functionally, however, C-ANF binding sites behave as if they are independent of B-ANF binding sites. Furthermore,

recent purification and sequence data of ANF receptors indicate that there are two biochemically distinct classes of ANF binding sites [J. Lewicki *et al.*, in *Proceedings and Abstracts of the Second World Congress of Biologically Active Atrial Peptides*, American Society of Hypertension, New York, 16–21 May 1987 (American Society of Hypertension, New York, 1987), p. 184]. Thus, C-ANF receptors are not simply “spare” receptors of a single class of ANF receptors.

13. F. A. Almeida, M. Suzuki, R. Scarborough, J. Lewicki, T. Maack, *ibid.*, p. 187.
14. Characterization of ANF receptors in kidney and other tissues by cross-linking techniques reveals lower molecular mass (= 40 to 70 kD) and higher molecular mass (= 120 to 180 kD) forms of the receptor [D. L. Schenk *et al.*, *J. Biol. Chem.* **260**, 14887 (1985); R. L. Vandler, K. E. Arkuri, M. A.

- Napier, *ibid.*, p. 10889; C. C. Yip, L. P. Laing, T. G. Flynn, *ibid.*, p. 8229; S. Meloche, H. Ong, M. Cantin, A. DeLean, *ibid.* **261**, 1525 (1986)].
15. F. C. Luft *et al.*, *J. Pharmacol. Exp. Ther.* **236**, 416 (1986).
16. V. Johnson and T. Maack, *Am. J. Physiol.* **233**, F185 (1977); T. Maack, *ibid.* **238**, F71 (1980).
17. M. J. F. Camargo *et al.*, *ibid.* **246**, F447 (1984).
18. M. J. F. Camargo, S. A. Atlas, T. Maack, *Life Sci.* **38**, 2397 (1986).
19. M. Epstein *et al.*, *J. Hypertension* **4** (suppl. 12), 593 (1986).
20. K. Horsky *et al.*, *Biochem. Biophys. Res. Commun.* **129**, 651 (1985).
21. Supported by NIH grant AM-14241 and by California Biotechnology, Inc., Mountain View, CA.

9 March 1987; accepted 29 July 1987

Identification of Putative Human T Cell Receptor δ Complementary DNA Clones

SHINGO HATA, MICHAEL B. BRENNER, MICHAEL S. KRANGEL

A novel T cell receptor (TCR) subunit termed TCR δ , associated with TCR γ and CD3 polypeptides, was recently found on a subpopulation of human T lymphocytes. T cell-specific complementary DNA clones present in a human TCR $\gamma\delta$ T cell complementary DNA library were obtained and characterized in order to identify candidate clones encoding TCR δ . One cross-hybridizing group of clones detected transcripts that are expressed in lymphocytes bearing TCR $\gamma\delta$ but not in other T lymphocytes and are encoded by genes that are rearranged in TCR $\gamma\delta$ lymphocytes but deleted in other T lymphocytes. Their sequences indicate homology to the variable, joining, and constant elements of other TCR and immunoglobulin genes. These characteristics, as well as the immunochemical data presented in a companion paper, are strong evidence that the complementary DNA clones encode TCR δ .

THE ANTIGEN-SPECIFIC RECEPTOR on the surface of most peripheral blood T lymphocytes is a disulfide-linked heterodimer composed of α and β subunits (40 to 50 kD), noncovalently associated with CD3 polypeptides (1–3). The TCR α and TCR β polypeptides are encoded by immunoglobulin-like variable (V), diversity (D), joining (J), and constant (C) gene segments that rearrange to form a functional gene during thymic T cell maturation (4–8). The TCR γ gene was identified as an additional immunoglobulin-like, T cell rearranging gene (9). Recently, 40- to 55-kD polypeptides encoded by functionally rearranged TCR γ genes were identified as one component of a heterodimer, associated with CD3 polypeptides, on populations of peripheral blood T lymphocytes (10), thymic T cells (11), and dendritic epidermal cells (12). The second component of the heterodimer appeared distinct from TCR γ and was proposed as a novel TCR subunit termed TCR δ .

Although little information is available concerning the biochemistry of the TCR δ protein, it might be supposed that it bears structural homology with other TCR subunits. This supposition leads to the prediction that TCR δ may be encoded by a gene that displays significant sequence homology to members of the immunoglobulin gene superfamily, that rearranges during T cell maturation, and that is expressed specifically in TCR $\gamma\delta$ T cells. Guided by these assumptions, we sought to obtain and characterize T cell-specific complementary DNA (cDNA) clones generated from messenger RNA (mRNA) of the human TCR $\gamma\delta$ cell line IDP2 (10).

A T cell-specific cDNA probe was generated by synthesizing ^{32}P -labeled first-strand cDNA of high specific activity from IDP2 polyadenylated [poly(A) $^+$] RNA, and subjecting this material to two cycles of hybridization with poly(A) $^+$ RNA from the human B cell line JY followed by hydroxylapatite chromatography (13). The twice subtracted single-stranded material was used to probe 40,000 plaques of an IDP2 $\lambda\text{gt}10$ cDNA library (14), and 391 (1%) hybridizing plaques were obtained. Subsequent analysis organized these clones into 14 cross-hybridizing groups, composed of as many as

139 and as few as 2 members. Three groups were identified as encoding TCR γ (10 members), TCR β (20 members), and CD3 δ/ϵ (7 members), as judged by hybridization with appropriate probes. Representative members of the remaining 11 groups (A,B,C,D,E,G,I,K,M,O,R) were labeled with ^{32}P and used to probe Northern blots. One group (O, consisting of six members) detected transcripts expressed in IDP2 and the TCR $\gamma\delta$ cell line PEER (15–17) but not expressed in JY and the TCR $\alpha\beta$ cell line HPB-ALL. On the basis of this result, two group O clones (O-240 and O-254) were selected for further study.

Northern blot analysis of a larger panel of RNA samples with O-240 as a probe (Fig. 1A) revealed the expression of cross-hybridizing transcripts in four TCR $\gamma\delta$ cell lines [IDP2, PEER, Molt-13 (18), and PBL L1 (16)]. Four distinct transcripts, of 2.2, 1.7, 1.3, and 0.8 kb (arrows in Fig. 1A), were detected. However, transcripts were undetectable in B cell line JY, myeloid cell line HL60, the TCR $\alpha\beta$ -bearing T cell line

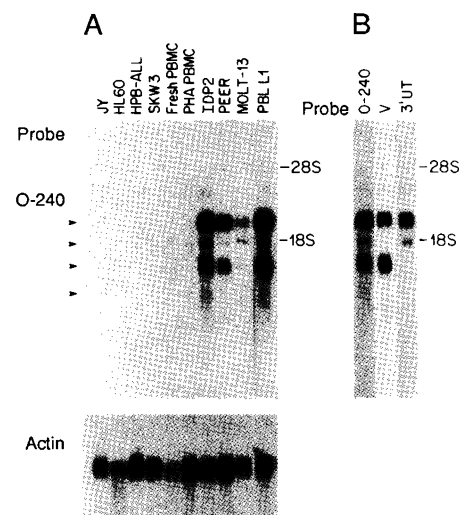


Fig. 1. Northern blot analysis of group O hybridizing transcripts. (A) Total RNA samples (5 μg) were electrophoresed through 1.5% agarose gels containing 2.2M formaldehyde, transferred to nitrocellulose, and probed with nick-translated O-240 or chicken actin (Oncor). Filters were washed with $1\times$ SSC and 0.5% SDS at 23°C and then with $0.1\times$ SSC at 50°C. RNA sources are: JY, B cell line; HL60, myeloid cell line; HPB-ALL and SKW3, TCR $\alpha\beta$ and surface TCR $^-$ T cell lines, respectively; fresh PBMC and PHA-PBMC, fresh and 2-day PHA-activated peripheral blood mononuclear cells; IDP2, PEER, Molt-13, and PBL-L1 [identical to WT31 $^-$ PBL line (16)] TCR $\gamma\delta$ T cell lines. (B) IDP2 RNA treated as above was probed with nick-translated O-240, a 240-bp EcoRI-Sca I fragment of O-240/38 (V probe; see Fig. 3A) labeled by hexanucleotide priming, or a 550-bp Hae III fragment of O-240 (3' UT; see Fig. 3A) labeled by nick-translation. Washing was as in (A). Arrowheads mark the positions of the four major transcripts detected; 18S and 28S ribosomal RNA served as markers.

S. Hata and M. S. Krangel, Division of Tumor Virology, Dana-Farber Cancer Institute, Harvard Medical School, Boston, MA 02115.

M. B. Brenner, Division of Tumor Virology, Dana-Farber Cancer Institute, and Department of Rheumatology and Immunology, Brigham and Women's Hospital, Harvard Medical School, Boston, MA 02115.